Biosci. Rep. (2011) / **31** / 87–98 (Printed in Great Britain) / doi 10.1042/BSR20100003

Original Paper

Hydrogen sulfide attenuates cardiac dysfunction in a rat model of heart failure: a mechanism through cardiac mitochondrial protection

Xianli WANG, Qian WANG, Wei GUO and Yi Zhun ZHU[1]

Department of Pharmacology, School of Pharmacy and Institute of Biomedical Sciences, Fudan University, Shanghai, People's Republic of China

Synopsis

HF (heart failure) after MI (myocardial infarction) is a major cause of morbidity and mortality worldwide. Recent studies have shown that hydrogen sulfide (H_2S) has cardioprotective effects. Hence, we aimed to elucidate the potential effects of H_2S on HF after MI in rats. The HF model after MI was made by ligating the left anterior descending coronary artery. HF groups and sham-operated groups of rats were treated with vehicle, sodium hydrosulfide (NaHS) or PAG (propagylglycine). Equal volumes of saline, 3.136 mg · kg^{-1} · day^{-1} NaHS or 37.5 mg · kg^{-1} · day^{-1} PAG, were intraperitoneally injected into rats for 6 weeks after operation. Survival, lung-to-body weight ratio and left ventricular haemodynamic parameters were measured. The protein and gene expression of Bcl-2, Bax, caspase 3 and cytochrome *c* were analysed by Western blotting and RT–PCR (reverse transcription–PCR). TUNEL (terminal deoxynucleotidyl transferase-mediated dUTP nick-end labelling) and EM (electron microscopy) were used to examine apoptosis of heart tissues. NaHS was found to improve the survival and lower the lung-to-body weight ratio. It increased the LVSP (left ventricular systolic pressure) and the maximum rate of pressure and decreased LVEDP (left ventricular end-diastolic pressure). Furthermore, NaHS promoted Bcl-2 protein and mRNA expression and demoted Bax, caspase 3 protein and mRNA expression in HF rats. We also showed that NaHS decreased the leakage of cytochrome *c* protein from the mitochondria to the cytoplasm. Histological observation by TUNEL and EM proved that NaHS inhibited cardiac apoptosis in HF hearts and improved mitochondrial derangements, but that PAG aggravated those indices. Hence, H_2S has protective effects in HF rats.

Key words: apoptosis, heart failure, heart function, hydrogen sulfide, mitochondria, myocardial infarction

INTRODUCTION

HF (heart failure) is a major cause of morbidity and mortality worldwide [1,2], and MI (myocardial infarction) is one of the most common causes of HF [3]. Apoptosis of cardiac myocytes is considered to be the main reason for HF. In many heart diseases such as MI, ischaemia/reperfusion injury or cardiomyopathy, cardiac myocyte apoptosis may be induced by molecular stimuli such as reactive oxygen species, angiotensin II, β_1-adrenergic agonists, pro-inflammatory cytokines and stretch [4]. If these diseases are not treated properly, heart function may be affected, eventually resulting in HF. Hence, interrupting the apoptosis of cardiac myocytes may increase the survival rate, ameliorate the impact of ventricular dysfunction and arrest the progression to HF. Hydrogen sulfide (H_2S), the third endogenous gaseous transmitter in mammals besides nitric oxide (NO) and carbon monoxide (CO), plays an important role in many organ systems [5–7]. In the cardiovascular system, H_2S is produced in the myocardium, fibroblasts and blood vessels from L-cysteine by the enzyme CSE (cystathionine γ-lyase). Most importantly, H_2S executes the physiological functions of vasorelaxation, cardioprotection [8,9] and inhibition of vascular remodelling. It is also brought into context with a variety of cardiovascular diseases such as spontaneous hypertension, hypoxia-induced pulmonary hypertension and high pulmonary blood flow-induced pulmonary hypertension [10].

Since its role in developing HF has not been investigated previously, the aim of the present study was to elucidate whether H_2S could attenuate ventricular dysfunction and arrest the progression of HF after MI.

Abbreviations used: CSE, cystathionine γ-lyase; DAB, diaminobenzidine; EM, electron microscopy; GAPDH, glyceraldehyde-3-phosphate dehydrogenase; HR, heart rate; HF, heart failure; LV, left ventricle; $+LV_{dp/dt}$, the maximum rate of pressure development; $-LV_{dp/dt}$, maximum rate of pressure decay over time; LVEDP, left ventricular end-diastolic pressure; LVSP, left ventricular systolic pressure; MI, myocardial infarction; PAG, propagylglycine; RT–PCR, reverse transcription–PCR; TUNEL, terminal deoxynucleotidyl transferase-mediated dUTP nick-end labelling.

[1]To whom correspondence should be addressed (email zhuyz@fudan.edu.cn or yizhunzhu@gmail.com).

MATERIALS AND METHODS

Animal care

Male Sprague–Dawley rats weighing 250–300 g were used for this experiment. The animals were housed under diurnal lighting conditions and fed standard rat chow and water *ad libitum*. All animal experiments were performed in accordance with the Animal Management Rules of the Ministry of Health of the People's Republic of China and approved by the Animal Research Ethics Committee, School of Pharmacy, Fudan University.

Drugs

PAG (propagylglycine) was purchased from Shanghai Intechem Technology, and sodium hydrosulfide (NaHS) was purchased from Sigma Chemical. Both drugs were dissolved in saline before intraperitoneal injection.

HF model and treatment protocols

MI was induced by ligation of the left anterior descending coronary artery approx. 2–3 mm from its origin, as described previously [11]. Briefly, the rats were anaesthetized with 7% chloral hydrate (3.5 mg/kg, intraperitoneal injection), endotracheally intubated and mechanically ventilated with room air at a respiratory rate of 100 breaths/min and a tidal volume of 2.5 ml with a rodent ventilator (DHX-150). Electrocardiography was recorded in the anaesthetized animal for a period of 1 min using the Animal Mflab200 amplifier. Under sterile conditions, a left thoracotomy was performed, and the fourth intercostal space was exposed. The pericardium was opened, and the heart was removed from the thoracic cavity. The proximal left anterior descending coronary artery was ligated with a 6-0 atraumatic suture that was passed through the superficial layers of the myocardium. Successful ligation of the coronary artery was verified by the colour change immediately in the ischaemic area (anterior ventricular wall and the apex) of the heart and MI was confirmed by electrocardiography (ST-segment elevation was observed). The heart was returned to the chest cavity, the lungs were reinflated and the chest incision was closed. Sham-operated rats were prepared in the same manner except for the left coronary ligation. After completion of the surgical procedures, rats were removed from the ventilator and the endotracheal tube was removed. Operative mortality was approx. 45% due to acute sudden death within the first 48 h after surgery. The size of MI at 48 h that we measured in the preliminary experiments was $37.2 \pm 3.2\%$ by 1% TTC (2,3,5-triphenyltetrazolium chloride) as in the previous study [9]. Electrocardiography was recorded 48 h after the operation. Limb lead was evaluated. The animals that showed a large Q wave (>0.3 mV) in lead II were used in subsequent experiments.

Surviving rats from the MI model and sham-operated groups were randomly assigned to six treatment groups: (i) HF rats treated with equal volume of vehicle ($n = 20$), (ii) HF rats treated with NaHS ($3.136\ mg \cdot kg^{-1} \cdot day^{-1}$) ($n = 20$), (iii) HF rats treated with PAG ($37.5\ mg \cdot kg^{-1} \cdot day^{-1}$) ($n = 20$), (iv) sham-operated rats treated with vehicle ($n = 5$), (v) sham-operated rats treated with NaHS ($3.136\ mg \cdot kg^{-1} \cdot day^{-1}$) ($n = 5$) and (vi) sham-operated rats treated with PAG ($37.5\ mg \cdot kg^{-1} \cdot day^{-1}$) ($n = 5$). During the treatment periods, cages were inspected daily for rats that had died. Treatment was continued for 6 weeks until haemodynamic measurements and sample collection had taken place.

Measurements of haemodynamic parameters

At 6 weeks after the operation, 7% chloral hydrate (3.5 mg/kg, intraperitoneal injection) was injected. The HR (heart rate), LVSP (left ventricular systolic pressure), LVEDP (left ventricular end-diastolic pressure), $+LV_{dp/dt}$ (the maximum rate of pressure development) and $-LV_{dp/dt}$ (maximum rate of pressure decay over time) of sham-operated and HF rats with vehicle, NaHS and PAG treatments were measured by methods described previously [11]. During chloral hydrate anaesthesia, a cannula with a heparinized PP10 in PP50 catheter was inserted into the LV (left ventricle) through the right common carotid artery. The catheter was connected to a pressure transducer. The pressure transducer was connected to a Powerlab data recording system (MFLab 200, AMP 20020830, Image analysis system). The indices of haemodynamic parameters, such as HR, LVSP, LVEDP, $+LV_{dp/dt}$ and $-LV_{dp/dt}$, were measured.

Morphological assessment of HF

After completing the measurements of haemodynamic parameters, the hearts and lungs were extracted for further examination. The lung-to-body weight ratio that serves as an index for pulmonary oedema after HF was determined ($n = 5$ per group). Hearts were carefully dissected by separating the LV (left ventricular free wall and interventricular septum) from the atria and right ventricle, followed by immediate freezing in liquid nitrogen and storage at –80 °C until extraction of total RNA [12]. The LVs were used for determining mRNA and protein levels.

Analysis of LV fibrosis after MI

Rat heart tissues ($n = 1$ for the sham group, $n = 3$ for each HF group) were fixed in 4% formalin overnight, dehydrated and finally embedded in paraffin. The embedded tissues were then cut into 5 μm slices and stained with the histological stain Picric Sirius Red, which distinguishes the fibrosis part (red) from non-fibrosis myocardial tissue (yellow). Images of the sectioned tissues were captured using an image analysis program for fibrosis size analysis, namely UTHSCSA ImageTool.

Measurement of H_2S concentration from plasma

H_2S concentrations were measured in plasma taken after 6 weeks of treatment ($n = 5$ per group). In brief, plasma from rat blood was collected and centrifuged prior to the animals being killed. Subsequently, 75 μl of the plasma sample was mixed with 250 μl of 1% zinc acetate and 425 μl of distilled water in a 1.5 ml Eppendorf tube. Subsequently, 133 μl of 20 mM

N-dimethyl-*p*-phenylenediamine sulfate was added in 7.2 mM HCl and 133 μl of 30 mM $FeCl_3$ in 1.2 mM HCl, and the reaction mixture was then incubated at room temperature (25 °C) for 10 min. The protein pellet in the reaction mixture was extracted by adding 250 μl of 10% trichloroacetic acid and centrifugation at 32 900 ***g*** for 5 min. The attenuance (*D*) of the resulting solution at 670 nm was assayed in a 96-well plate and measured using a spectrophotometer (TECAN Systems). All samples were assayed in duplicate, and the concentrations of each sample were calculated against a calibration curve using NaHS (3.125–250 μM). Plasma H_2S concentration in μM is presented as previously reported [9,13,14].

Separation of cytosolic protein and mitochondrial protein

Isolation of mitochondria protein from left ventricular tissue was performed according to the manufacturer's protocol (Beyotime, Nantong, China). The tissues ($n = 4$ per group) were washed twice with ice-cold PBS, resuspended in lysis buffer (20 mM Hepes/KOH, pH 7.5, 10 mM KCl, 1.5 mM $MgCl_2$, 1.0 mM sodium EDTA, 1.0 mM sodium EGTA, 1.0 mM dithiothreitol, 0.1 mM PMSF and 250 mM sucrose) and then homogenized by an autohomogenizer in ice/water. After removing the nuclei and cell debris by centrifugation at 1000 ***g*** for 10 min at 4 °C, the supernatants were further centrifuged at 10 000 ***g*** for 10 min at 4 °C. The resulting mitochondrial pellets were resuspended in lysis buffer. The supernatants from the 10 000 ***g*** centrifugation were centrifuged once more at 100 000 ***g*** for 1 h at 4 °C and then collected. The supernatants and mitochondrial fractions were stored at –80 °C. Proteins from the cytoplasm and mitochondria were used to measure the leakage of cytochrome *c*.

Total protein extraction from left ventricular tissue

Frozen tissues ($n = 4$ per group) were cut into small pieces and homogenized in 0.5 ml of RIPA buffer (150 mM NaCl, 1% Nonidet P40, 0.5% deoxycholate, 0.1% SDS, 50 mM Tris/HCl and 2 mM PMSF, pH 7.4) prior to being transferred into small tubes and rotated at 4 °C overnight. Solubilized proteins were collected after centrifugation at 10 000 ***g*** for 30 min. The supernatant was collected and stored at –80 °C. Those whole cell proteins were used to test the expression of CSE and apoptotic factors such as Bcl-2, Bax and caspase 3.

Western-blot analysis of proteins in left ventricular tissue

The protein concentration of each sample was quantified using the enhanced BCA (bicinchoninic acid) Protein Assay kit (Beyotime Biotechnology, Haimen, China). To detect CSE, Bcl-2, Bax, cytochrome *c* and caspase 3 protein levels, protein lysates from each group of rats were separated by SDS/PAGE and electrotransferred on to a PVDF membrane (Millipore). Polyacrylamide gels (12%) were used for CSE (43 kDa) and pro-caspase 3 (32 kDa) protein testing. For Bcl-2 (29 kDa), Bax (21 kDa), cytochrome *c* (15 kDa) and cleaved caspase 3 (17 kDa) protein expression, 15% (w/v) polyacrylamide gels were used. The non-specific proteins on membranes were blocked with 5% non-fat dried skimmed milk powder prepared in TBS+0.1% Tween 20 for 2 h at room temperature. Immunoblotting was then performed using 2 μg/ml rabbit anti-rat CSE polyclonal antibody (R&D Systems), rabbit anti-rat Bcl-2 and Bax polyclonal antibodies (Santa Cruz Biotechnology), rabbit anti-human caspase 3 polyclonal antibody (Santa Cruz Biotechnology) and mouse anti-horse cytochrome *c* monoclonal antibody (Santa Cruz Biotechnology) respectively. Membrane blots were washed and incubated with horseradish-peroxidase-conjugated anti-rabbit IgG antibodies or anti-mouse IgG antibodies at a 1:10000 dilution (Jackson ImmunoResearch Laboratories). Immunoreactive proteins were then visualized using ECL® plus, a Western blotting detection system (Alpha Innotech).

Total RNA isolation and RT–PCR (reverse transcription–PCR)

Total RNA from non-infarcted left ventricular tissue ($n = 4$ per group) was extracted using TRIzol® reagent according to the manufacturer's instructions. RNA was spectrophotometrically quantified by measuring the absorbance of samples at 260 nm/280 nm and then re-dissolved in 30–50 μl of DEPC (diethyl pyrocarbonate)-treated water (mRNA concentration of each sample was 50 ng/μl) and stored at –80 °C. Then, 2 μg of mRNA was reversed-transcribed to cDNA with a PrimeScript™ 1st Strand cDNA Synthesis kit and stored at –20 °C. RT–PCR was performed in a 0.2 ml tube with a total sample volume of 25 μl containing 2 μl of tissue cDNA, 1 μl of 5 μM per primer mixture, 1 μl of 2.5 mM per dNTP mixture, 1.5 μl of 1.5 mM $MgCl_2$, 2.5 μl of 10 × PCR buffer and 1.25 units of Taq DNA polymerase. The gene encoding GAPDH (glyceraldehyde-3-phosphatase dehydrogenase) was considered as an internal standard. PCR was run at 35 cycles for GAPDH, CSE and caspase 3 and at 40 cycles for Bax and Bcl-2. Reverse transcription action was performed at 50 °C for 30 min. Samples were then heated to 95 °C for another 15 min for the initial PCR activation step. Three-step PCR began with denaturation at 94 °C for 30 s, followed by 30 s of annealing for GAPDH, CSE, Bcl-2 and caspase 3 at 56 °C and for Bax at 57 °C and then continued with an extension at 72 °C for 1 min. A final extension was carried out at 72 °C for 15 min. The PCR products were separated electrophoretically on a 1.5% agarose gel and stained with ethidium bromide. The absorbance of the band of each mRNA was measured by using the Fluor Chem SP system. Primer preparations were devised in accordance with GenBank® Nucleotide Sequence Database. The nucleotide sequences of the primers used in the present study are shown in Table 1.

TUNEL (terminal deoxynucleotidyl transferase-mediated dUTP nick-end labelling) assay

The TUNEL assay was used to test the apoptosis of cardiomyocytes in rat hearts. The heart tissues ($n = 1$ for sham group and $n = 3$ for each HF group) were fixed in 4% formalin overnight, dehydrated and then embedded in paraffin. The tissues were cut

Table 1 Primers was used in the present study

Gene	GenBank® accession no.	Nucleotide sequence	Product size (bp)
CSE	AY641456		201
Sense		5′- TCCGATGACCTCAACGAAC -3′	
Antisense		5′-CGGTAGCCCAGGATAAATAA-3	
Caspase 3	NM012922		102
Sense		5′-CTGGACTGCGGTATTGAG-3′	
Antisense		5′-GGGTGCGGTAGAGTAAGC-3	
Bcl-2	NM 016993		422
Sense		5′-CGGGAGATCGTGATGAAGT-3′	
Antisense		5′-CCACCGAACTCAAAGAAGG-3′	
Bax	NM007527		579
Sense		5′-GCAGGGAGGATGGCTGGGGAGA-3	
Antisense		5′-TCCAGACAAGCAGCCGCTCACG-3′	
GAPDH	NM017008		578
Sense		5′-TTCAACGGCACAGTCAAGG-3′	
Antisense		5′-CGGCATGTCAGATCCACAA-3′	

into 7 μm thick slices. The assay was tested by a TdT-FragEL™ DNA Fragmentation Detection kit acquired from Calbiochem, and the empirical procedure was performed according to the kit's protocol.

Morphological change in the myocardium

Ultrastructural apoptosis of cardiomyocytes in our present study was detected by EM (electron microscopy). Samples were taken at the peri-infarct site in three rats from each group. Samples for EM were cut into pieces less than 1 mm^3 and fixed in 2.5% glutaraldehyde in 0.1 M sodium cacodylate buffer (pH 7.4) for 4 h. Tissues were post-fixed in 1% osmium tetroxide in 1% $K_4Fe(CN)_6$ buffered with 0.1 M sodium cacodylate, dehydrated through graded concentrations of ethanol and propylene oxide and subsequently embedded in Epon 812. Ultrathin sections were cut from blocks and mounted on copper grids. Then, the grids were counterstained with lead citrate and uranyl acetate. The sections were observed with a Philips CM 120 electron microscope.

Statistical analysis

Data are expressed as means ± S.E.M. All data involving multiple groups were analysed by one-way ANOVA. Differences between individual groups were analysed using the Student's *t* test. Survival rate was analysed by the Kaplan–Meier analysis using the log-rank test. A difference with $P < 0.05$ was considered statistically significant.

RESULTS

Survival rate

Total mortality during the observation periods from the first to sixth week in rats subjected to coronary ligation was 2/20 NaHS, while vehicle was 5/20 and PAG was 8/20. During the 6-week observation period, none of the sham-operated animals died. The survival rate among NaHS-treated ligated rats (90%) was significantly high compared with the vehicle-treated group (75%) and the PAG-treated group (60%) ($P < 0.05$). This significant difference in survival rate was not due to differences in infarct size because the rats were randomly grouped 48 h after MI (Figure 1).

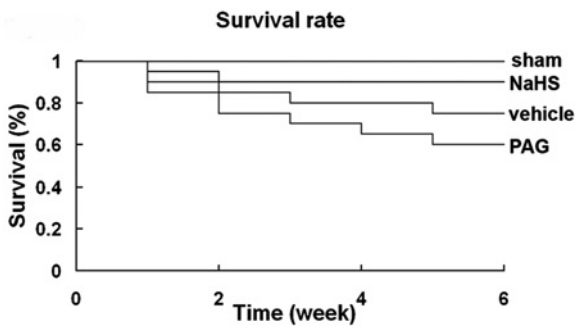

Figure 1 The Kaplan–Meier survival plot
A survival plot demonstrating a significant reduction in overall mortality in the NaHS-treated group (2/20) compared with vehicle-treated animals (5/20), and the PAG-treated group (8/20) had a higher mortality rate compared with vehicle-treated animals ($P < 0.05$).

Effects on left ventricular haemodynamic parameters

LVSP in PAG-treated HF rats (107 ± 2.2 mmHg; 1 mmHg = 0.133 kPa) was lower compared with vehicle-treated HF rats (119 ± 3.1 mmHg, $P < 0.05$), and it was even lower compared with NaHS-treated HF rats (132 ± 1.8 mmHg, $P < 0.01$). The LVSP of NaHS-treated HF rats is higher than that of vehicle-treated HF rats ($P < 0.05$). The LVEDP was increased in PAG-treated HF rats (18 ± 0.9 mmHg) compared with vehicle-treated HF rats (14 ± 0.9 mmHg, $P < 0.05$); it was also higher than that

Table 2 Haemodynamic parameters of HF and sham rats at the sixth week after the operation ($n = 5$ for each sham group and $n = 8$ for each HF group)
In model group, *vehicle versus NaHS, $P < 0.05$; †vehicle versus PAG, $P < 0.05$; ‡sham versus model + vehicle, $P < 0.05$.

	Sham			Model		
	Vehicle	NaHS	PAG	Vehicle	NaHS	PAG
HR (beat/min)	438 ± 13	407 ± 14	430 ± 19	439 ± 15	437 ± 15	437 ± 14
LVSP (mmHg)	137 ± 1.3	139 ± 1.7	135 ± 1.3	119 ± 3.1†	132 ± 1.8*	107 ± 2.2†
LVEDP (mmHg)	3.3 ± 0.3	3 ± 1	4 ± 1.2	14 ± 0.9†	10 ± 0.9*	18 ± 0.9†
$LV_{+dp/dt}$ (1000 mmHg/s)	6.6 ± 0.2	5.9 ± 0.3	6.0 ± 0.1	4.4 ± 0.5†	5.8 ± 0.2*	3.2 ± 0.2
$LV_{-dp/dt}$ (1000 mmHg/s)	5.4 ± 0.2	5.0 ± 0.5	5.2 ± 0.4	3.5 ± 0.1†	4.9 ± 0.4*	3.1 ± 0.2

of NaHS-treated HF group (10 ± 0.9 mmHg, $P < 0.05$). The decrease in $LV_{+dp/dt}$ in HF rats was significantly increased by NaHS treatment (5.8 ± 0.2 1000 mmHg/s). The aggravated $LV_{-dp/dt}$ was also improved in NaHS-treated HF group (4.9 ± 0.4 1000 mmHg/s). The significant changes of LVSP, LVEDP and $LV_{\pm dP/dt}$ indicated that H_2S could improve cardiac function of post-infarction HF. The heart rate in HF and sham-operated rats was not affected by treatment with NaHS and PAG (shown in Table 2). Furthermore, the results indicate that long-term treatments with NaHS and PAG could not affect the left ventricular haemodynamic parameters in sham-operated rats, although it showed a significant pharmacological effect in pathological conditions (like HF).

Effects on pulmonary oedema after 6 weeks of treatment

Figure 2 illustrates the ratio of lung weight to body weight for HF and sham-operated rats. Compared with sham rats, the lung-to-body weight ratio was higher in HF rats, $P < 0.05$. NaHS treatment significantly lowered the lung-to-body weight ratio in HF rats (6.0 ± 0.2 mg/g versus 9.2 ± 0.5 mg/g in vehicle HF, $P < 0.05$), and PAG HF (15.6 ± 2.1 mg/g) had a much high ratio compared with vehicle HF ($P < 0.05$). The result indicates that H_2S attenuates the degree of pulmonary oedema during HF. In sham groups treated with NaHS, saline and PAG, the ratio was 4.9 ± 0.1, 4.3 ± 0.6 and 5.4 ± 0.1 mg/g respectively and there was no statistical difference.

Result of analysis for LV fibrosis after MI

Fibrosis size was documented as percentage of fibrosis area compared with total left ventricular area in representative sections. The fibrosis size/total area of LV was significantly less in rats subjected to NaHS treatment than in vehicle-injected rats (12.5 ± 0.5% versus 25.7 ± 1.2%; $P < 0.01$). However, fibrosis size was greater (37.3 ± 0.9%; $P < 0.05$) in the PAG-treated animals (Figure 3).

Plasma H_2S levels in each group after 6 weeks of treatment

In the NaHS-treated HF group, plasma H_2S concentration was significantly increased to 69.5 ± 4.6 μM when compared with

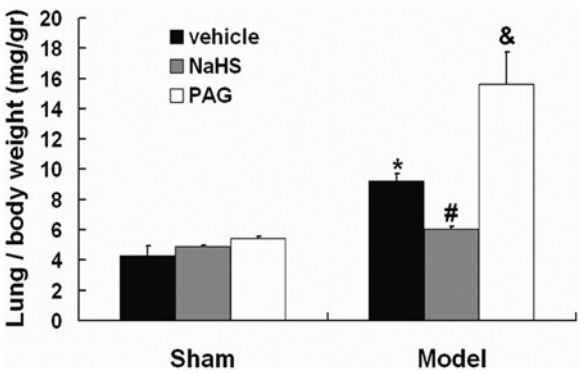

Figure 2 Effect of long-term treatment with NaHS and PAG on change in lung-to-body weight ratio of HF and sham-operated rats
#NaHS-treated HF group versus vehicle-treated group, $P < 0.05$. &Vehicle-treated group versus PAG-treated group, $P < 0.05$. *Vehicle-treated HF group versus vehicle sham group, $P < 0.01$.

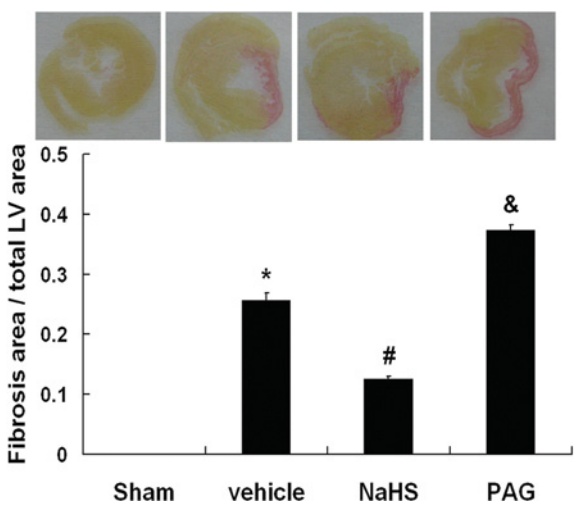

Figure 3 Myocardial fibrosis size change in vehicle-, NaHS- and PAG-treated animals
#NaHS-treated HF versus vehicle-treated HF, $P < 0.05$. &Vehicle-treated HF group versus PAG-treated HF group, $P < 0.05$. *Vehicle-treated HF versus vehicle sham, $P < 0.001$.

PAG-treated HF group whose plasma H_2S concentration was 45.8 ± 1.1 μM, $P < 0.01$, $n = 8$. The concentration in

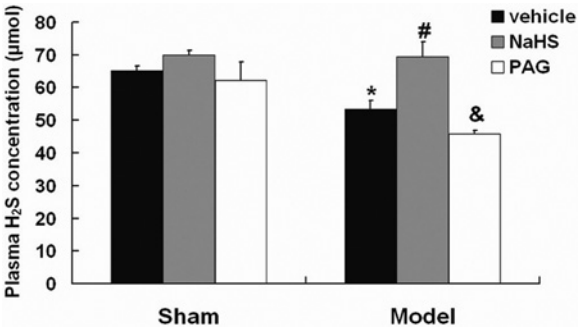

Figure 4 Effect of long-term treatment with 3.136 mg/kg NaHS and 37.5 mg/kg PAG on change in plasma H_2S concentration of HF and sham-operated rats

[#]NaHS-treated HF group versus vehicle-treated group, $P < 0.05$. [&]Vehicle-treated group versus PAG-treated group, $P < 0.05$. *Vehicle-treated HF group versus sham group, $P < 0.05$.

saline-treated HF group was 53.3 ± 2.7 μM, $P < 0.05$, compared with the other two HF groups. In sham-operated groups, however, the plasma H_2S level of rats was observed as follows: PAG+sham (62.1 ± 5.7 μM), NaHS+sham (69.9 ± 1.5 μM), saline+sham (65.1 ± 1.5 μM). They were all slightly higher than their model groups, but it had no statistical significance (Figure 4). Combining the results of survival rate, heart function, lung-to-body weight ratio and plasma H_2S concentration, it was determined that NaHS and PAG could not change the physiological function and plasma H_2S level in normal rats; therefore, these two sham groups were not included in the subsequent studies.

Measurement of protein level in left ventricular tissue

Western blotting was utilized to detect the protein levels of total CSE and Bcl-2, Bax, cytochrome *c*, pro- and cleaved caspase 3. The CSE protein content in the NaHS-treated HF group (0.66 ± 0.04) was higher than vehicle-treated HF group (0.51 ± 0.03) with a statistical significance of $P < 0.05$. PAG-treated HF group showed a decreased CSE protein expression (0.36 ± 0.02, $P < 0.05$) when compared with vehicle-treated HF group. This showed that NaHS could stimulate the expression of CSE in LV after MI. Bcl-2 protein content in the NaHS-treated HF group (1.64 ± 0.09) was higher than in the vehicle-treated HF group (1.12 ± 0.12, $P < 0.05$), which was also higher than in the PAG-treated HF group (0.64 ± 0.04, $P < 0.05$). The Bax protein content in the NaHS-treated HF group (0.61 ± 0.12) was the lowest among the vehicle-treated HF group (0.93 ± 0.06; $P < 0.05$) and the PAG-treated HF group (1.44 ± 0.18; $P < 0.05$) (Figure 5). The ratio of mitochondria cytochrome *c* and the cytoplasm cytochrome *c* indicated that the NaHS-treated group had low leakage of cytochrome *c* from the mitochondria to the cytoplasm

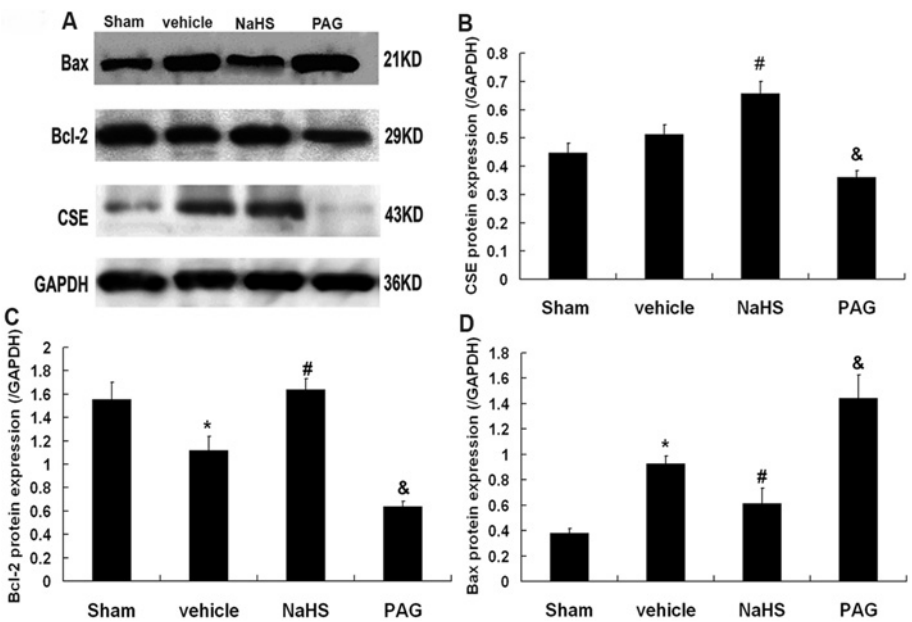

Figure 5 Cardiac protein expression in LV using the Western-blot method

(**A**) SDS/PAGE analysis shows CSE, Bcl-2 and Bax protein levels in LV of rats after a 6 week treatment, (**B**) change of CSE protein expression, (**C**) change of Bcl-2 protein expression and (**D**) change of Bax protein expression. [#]NaHS-treated HF versus vehicle-treated HF group, $P < 0.05$. [&]Vehicle-treated HF group versus PAG-treated HF group, $P < 0.05$. *Vehicle-treated HF versus vehicle sham group, $P < 0.05$.

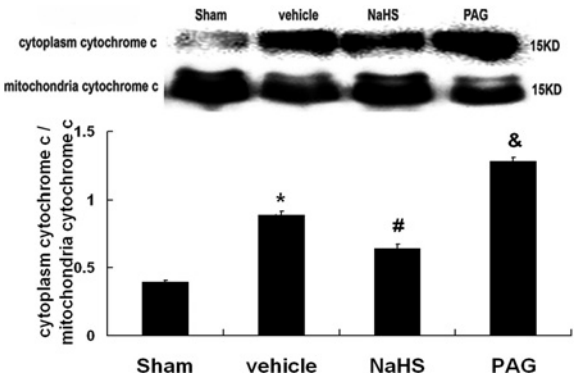

Figure 6 Leakage of cytochrome c protein from the mitochondria to the cytoplasm using the Western-blot method

*Vehicle-treated HF versus vehicle sham group, $P < 0.05$. #NaHS-treated HF versus vehicle-treated HF group, $P < 0.05$. &Vehicle-treated HF group versus PAG-treated HF group, $P < 0.05$.

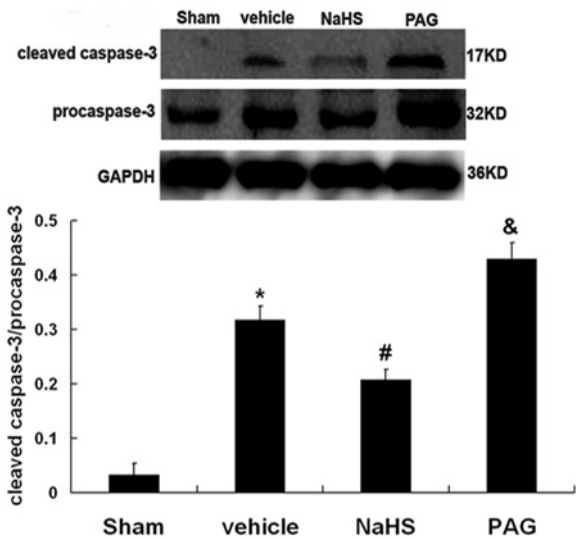

Figure 7 Activation of caspase 3 from pro-caspase 3 (32 kDa) to cleaved caspase 3 (17 kDa) using the Western-blot method

*Vehicle-treated HF versus vehicle sham group, $P < 0.05$. #NaHS-treated HF versus vehicle-treated HF group, $P < 0.05$. &Vehicle-treated HF group versus PAG-treated HF group, $P < 0.05$. KD, kDa.

compared with the vehicle-treated group ($P < 0.05$), which also had lower leakage than the PAG-treated group ($P < 0.05$; Figure 6). The results also showed a significant increase in activation of caspase 3 in HF hearts by comparing the intensities of cleaved with uncleaved caspase 3 fragments (Figure 7). The cleavage of caspase 3 in normal hearts was negligible ($3.25 \pm 2.1\%$) compared with $31.8 \pm 2.5\%$ in the vehicle-treated HF group. And NaHS treatment lowered the activation of caspase 3 in failing hearts ($20.1 \pm 2.1\%$), whereas PAG increased the activation to $43 \pm 2.9\%$ ($P < 0.05$, versus vehicle-treated HF group).

Measurement of gene expression in ventricular myocardium

To further verify the changes after post-infarction HF, the gene expression of CSE and Bcl-2, Bax and caspase 3 mRNA were assayed by RT–PCR (Figure 8). In the model group, CSE gene expression was significantly higher in NaHS-treated HF group (0.94 ± 0.03) when compared with the vehicle-treated HF group (0.72 ± 0.03; $P < 0.05$). The PAG-treated HF group (0.52 ± 0.01) showed lower CSE gene expression than the vehicle-treated HF groups ($P < 0.05$). The expression of pro-apoptotic genes such as Bax and caspase 3 were found to be lower after treatment with NaHS when compared with treatment with vehicle ($P < 0.05$). However, Bcl-2 gene expression was remarkably suppressed after treatment with PAG (1.25 ± 0.31) compared with treatment with vehicle (1.75 ± 0.51; $P < 0.05$). Furthermore, treatment of NaHS could increase the expression of the Bcl-2 gene (2.28 ± 0.22) compared with the vehicle-treated group. Those results correlate with the observation of protein changes in the same treatment groups.

Result of the TUNEL assay

The results were detected through a light microscope; a dark brown DAB (diaminobenzidine) signal indicated positive staining, while shades of blue-green to greenish tan signified a non-reactive cell. Since the 3′-OH ends of DNA fragments generated by apoptosis were concentrated within the nuclei and apoptotic bodies, morphology as well as DAB staining could be used to interpret FragEL^{TM} results. Non-apoptotic cells did not incorporate significant amounts of labelled nucleotide, since they lacked an excess of 3′-OH ends and should be dominantly rounded and appear counterstained with Methyl Green. This further explained that more brown nuclei represented more apoptotic cells in heart tissues. In Figure 9(A), a few of the brown nuclei are found in the sham group heart, while the number of brown nuclei increased significantly in model groups. The NaHS treatment could attenuate the number of apoptotic cells. By contrast, PAG increased cardiomyocyte apoptosis. Cells with brown nuclei and total nuclei in the peri-infarcted area for five visual fields in a section were counted, and there were four sections for each group. The ratio for the number of brown nuclei in the total nuclei was also calculated. The result had statistical significance and is shown in Figure 9(B).

Morphological change in the myocardium after 6 weeks of treatment

After 6 weeks treatment, the rat heart sections were examined by EM. There was no evidence of apoptosis in the sham-operated rat. A normal cardiomyocyte is shown in Figure 10. Finely granular chromatin was present. Mitochondria showed regular cristae. A normal arrangement of sarcomeres was also evident. In the vehicle-treated model group, the consistent presence of mitochondrial derangements was examined. Mitochondria appeared to be swollen with disorganized cristae and formation of wrinkled bodies. Loss of normal striations and disorganization

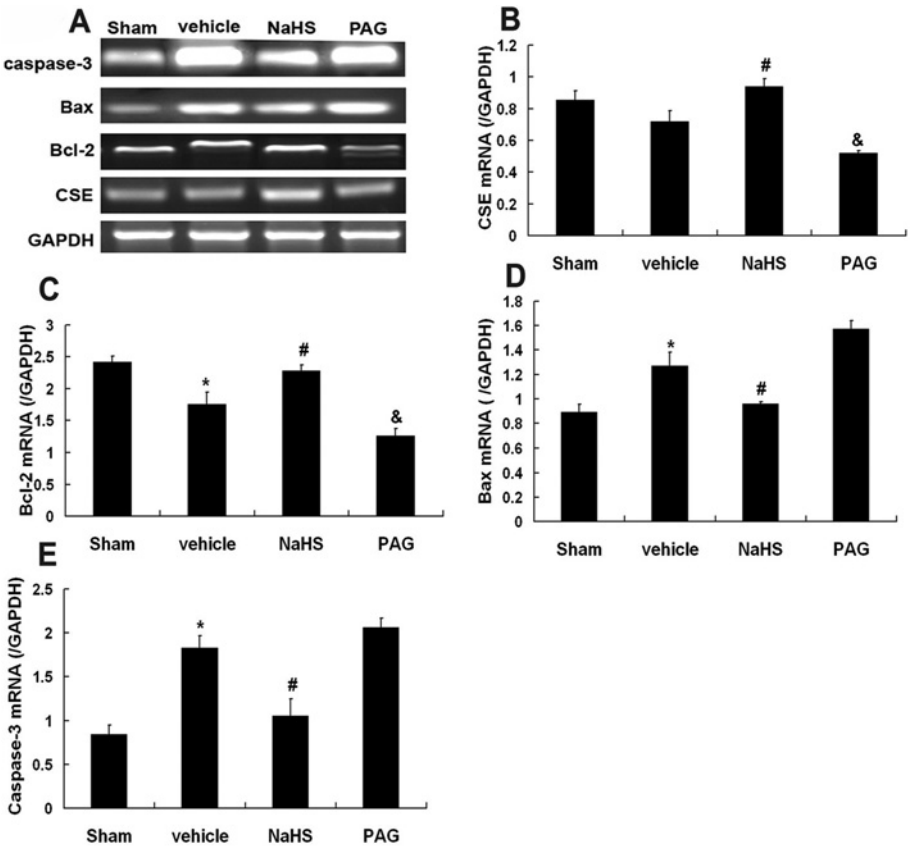

Figure 8 Cardiac gene expression in LV using the RT–PCR method

(**A**) Ethidium bromide–agarose gel showing CSE, Bcl-2, Bax and caspase 3 mRNA levels in LV after a 6-week treatment. (**B**) Detecting CSE gene expression. (**C**) Detecting Bcl-2 gene expression. (**D**) Detecting Bax gene expression. (**E**) Detecting Caspase 3 gene expression. #NaHS-treated HF versus vehicle-treated HF, $P < 0.05$. &Vehicle-treated HF versus PAG-treated HF, $P < 0.05$. *Vehicle-treated HF versus vehicle sham, $P < 0.05$.

of sarcomeres were also found, and the shape of the nuclei was abnormal. However, the NaHS-treated group had slight swollen mitochondria, disorganized cristae and myofibrillar derangements. The PAG-treated group showed severe mitochondrial derangement and myofibrillar derangements, and nuclei condensation was apparent.

DISCUSSION

H_2S has been studied intensively in recent years; it is synthesized endogenously in various mammalian tissues by two pyridoxal-5′-phosphate-dependent enzymes responsible for metabolizing L-cysteine: CBS (cystathionine β-synthase) and CSE. CSE is a major H_2S-producing enzyme in the cardiovascular system. A study has highlighted protective effects of H_2S on cardiac myocyte injury during isoprenaline-induced MI [15]. Similarly, NaHS was observed to limit the size of infarction induced by left coronary artery ligation. In addition, NaHS also has been shown to protect cultured myocardial cells against hypoxia-induced cell death [8].

The recent discovery of the novel effects of H_2S on physiological functions such as vasodilation [16] and neuromodulation [17,18] has suggested possible roles for this gas in cardiovascular and neurological diseases. Moreover, H_2S also plays a key role in the pathophysiology of endotoxin, septic and haemorrhagic shock [13], vasorelaxation [19], inflammation [14,20] and cardiac function in rats [21].

In the present study, NaHS was used as an H_2S donor, which was dissolved in water; HS^- is released and forms H_2S with H^+. This provides a solution of H_2S at a concentration that is approx. 33% of the original concentration of NaHS [22]. We found that long-term treatment with NaHS in the model group promoted a significant increase in the H_2S plasma levels when compared with the vehicle group and PAG group. This observation corresponds to the up-regulation of the expression of CSE mRNA and protein

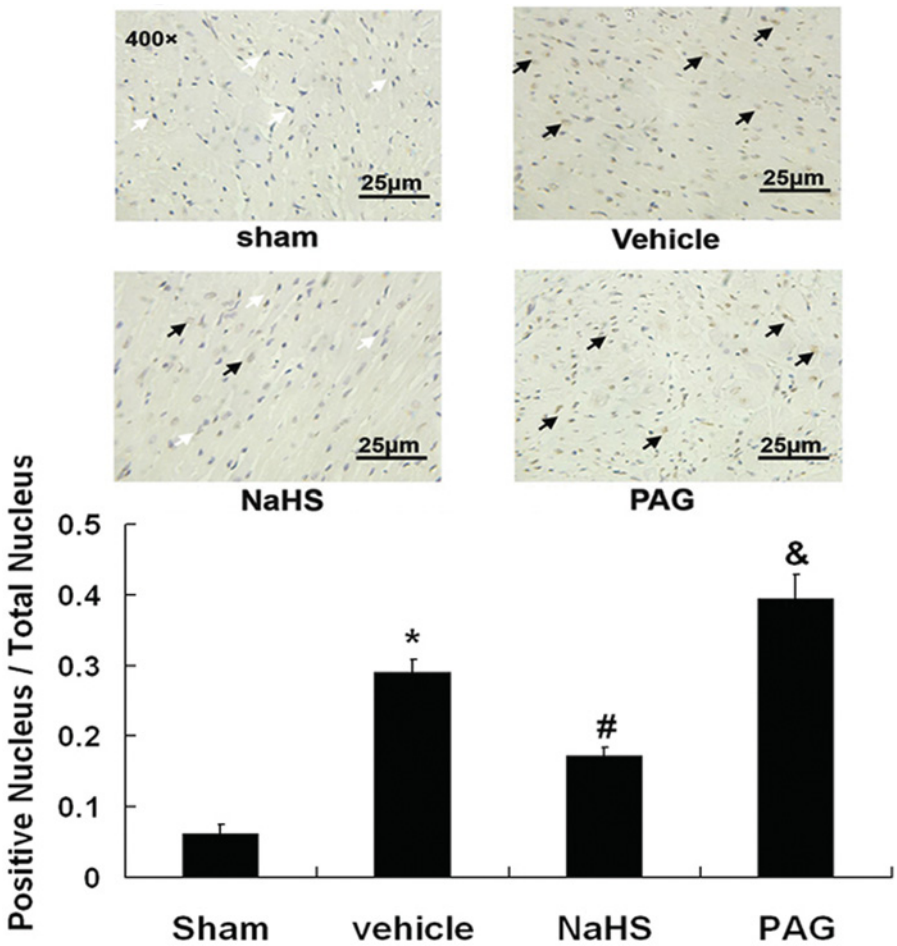

Figure 9 TUNEL analysis for apoptosis cells

↗ (white) show normal blue nucleus; ↗ (black) indicate apoptotic nucleus in brown. *Vehicle-treated HF versus vehicle sham, $P < 0.05$. #NaHS-treated HF versus vehicle-treated HF, $P < 0.05$. &Vehicle-treated HF group versus PAG-treated HF group, $P < 0.05$.

in myocardial tissues. While we noted that both NaHS and PAG affected little the concentration of plasma H_2S for sham groups, this led us to hypothesize that, under physiological conditions, the H_2S level in plasma may keep its balance by its autoregulation.

The haemodynamic measurements were improved in the NaHS-treated HF group compared with the vehicle and PAG HF groups by increasing $LV_{\pm dp/dt}$ and LVSP, while decreasing LVEDP. These parameters indicate that the decrease in myocardial function was improved in the NaHS-treated HF rats. Thus the increase in survival rate is associated with improvement of the haemodynamic function of rats with coronary artery ligation. We also found that NaHS decreased the fibrosis size compared with the vehicle HF group, and PAG treatment enlarged the size. All these show the beneficial long-term effects of H_2S on the haemodynamic parameters of the pathophysiological changes in developing HF.

Heart rate in rats with coronary artery ligation and sham rats was not affected by treatment. This finding is in agreement with other studies showing that the heart rate remained essentially unchanged after completing the study of the post-infarction HF rats [23,24]. In view of the unchanged heart rate after the coronary artery ligation, it appears that the maintenance of high output status at early stages relied on the Frank–Starling reserve and the intact contractile function [24].

The decrease in $LV_{\pm dp/dt}$, LVSP and the increased LVEDP indicate the presence of LV dysfunction in developing HF groups. Although the permanent occlusion model for HF will have some limitations such as high risk of operation and high mortality in the acute period compared with the adriamycin or isoprenaline model, it is still in common usage in long-term research today [25].

Many heart diseases such as myocardial ischaemia/reperfusion injury and MI result in the robust appearance of cardiac myocyte apoptosis, which contributes to infarct size and long-term ventricular dysfunction [26–28]. Rescue from apoptotic cell death through the interference of the central programmed death

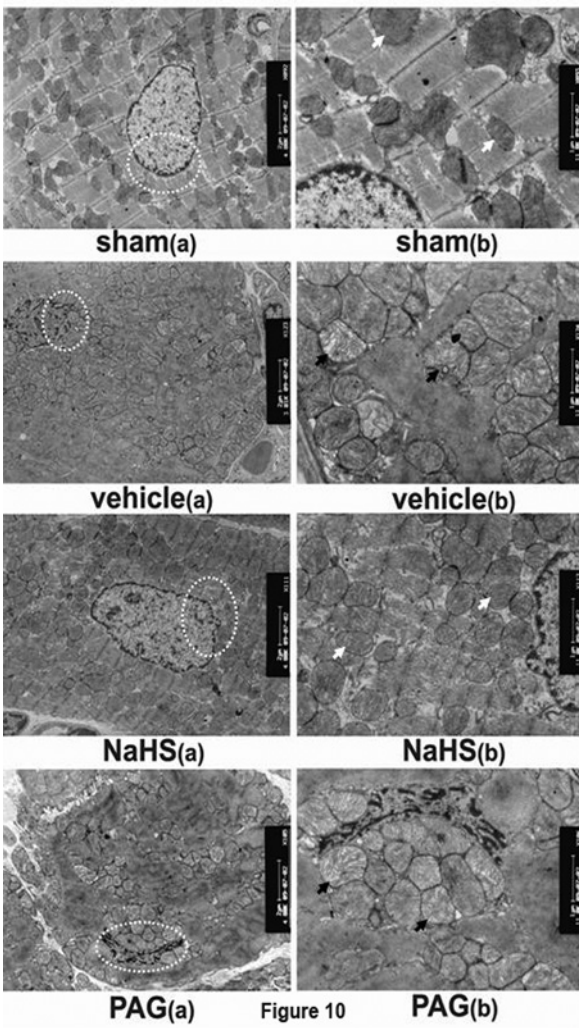

Figure 10 Ultrastructure changes in the peri-infarct area of rat heart with EM (×20000)

(**a**) This Figure shows low magnification for each group; (**b**) this Figure shows higher magnification of the area for each group. ↗ (white) shows normal mitochondrial; ↗ (black) indicates swelling mitochondria and some mitochondria with ruptured outer membrane. In the sham group, mitochondria show regular cristae. Normal arrangement of sarcomeres is also evident. In the vehicle-treated model group, mitochondrial derangements were always present. Mitochondria appeared swollen, with disorganized cristae and formation of wrinkled bodies, loss of normal striations and disorganization of sarcomeres were also found, and the nuclei shape was abnormal. While the NaHS-treated group had mitochondria slightly swollen, disorganized cristae and myofibrillar derangements, the PAG-treated group showed severe mitochondrial derangement and myofibrillar derangements, and nuclei condensation is apparent.

pathways, such as the knockout of the pro-apoptotic gene or loss-of-function mutation in the death receptor, consistently reduced infarct size after ischaemia/reperfusion injury by 50–60% [29] and may attenuate ventricular dysfunction, which confirms the importance of apoptosis in these models. Severity of cardiomyopathy after MI, ischaemia/reperfusion injury or aortic constriction is also reduced by inhibition of cardiac myocyte apoptosis [30,31]. It may also do the same to HF after MI. Some mouse models demonstrate that cardiac myocyte apoptosis itself can directly cause dilated cardiomyopathy and is sufficient to result in decreased survival [32]. Hence, the maintenance of cardiac myocyte numbers is critical to the overall preservation of both structural integrity and function of the heart. Similarly, pharmacological and transgenic studies in animal models indicate that the inhibition of cardiac myocyte apoptosis appears to ameliorate the impact of MI and thus arrests the progression to HF.

It is known that apoptosis is mediated by two inter-connected pathways [33]. The extrinsic or death receptor pathway transmitted death signals from relatively specialized ligands such as Fas ligand or TNFα (tumour necrosis factor-α). In contrast, the more ancient intrinsic or mitochondrial/ER (endoplasmic reticulum) pathway transducts a wide spectrum of death signals that originate both outside and inside the cell. These include deficiency in nutrients/survival factors/oxygen, oxidative stress, physical and chemical toxins (radiation and drugs), DNA damage and misfolded proteins. Stimulation of these pathways triggers the translocation of death-promoting proteins (e.g. cytochrome *c*) from the mitochondria to the cytoplasm [34] and the activation of a class of cysteine proteases called caspases. Caspases, in turn, bring about apoptotic death. In a study by Lefer and colleagues, it was reported that the H_2S attenuates myocardial ischaemia/reperfusion injury by preservation of mitochondrial function [35]. In a different study, it was reported that mitochondrial changes are prevalent in apoptosis of the myocardium [36]. Moreover, myofibrillar derangements are obviously peculiar to apoptotic cardiomyocytes, in keeping with the finding of caspase 3-dependent myofibrillar lysis. Therefore the morphological observation of apoptosis in cardiomyocytes was performed by EM in the present study, and the result showed that H_2S ameliorated mitochondrial derangements, such as swelling, disorganized cristae, loss of normal striations and attenuation of myofibrillar disorganization. The TUNEL test also showed that H_2S decreased the number of apoptotic cardiomyocytes.

The anti-apoptotic factor Bcl-2 and pro-apoptotic factors such as Bax, caspase 3 and cytochrome *c* in the LV were tested. The results showed that H_2S could increase the mRNA and protein expression of Bcl-2, decrease the mRNA and protein expression of Bax and caspase 3 and lower the mitochondrial cytochrome *c* release to the cytoplasm. In early apoptotic signalling, the anti-apoptotic Bcl-2 and pro-apoptotic Bax are in opposition. A shift in favour of the pro-apoptotic proteins subsequently results in increased mitochondrial pore permeability, releasing cytochrome *c* and apoptosis-inducing factor, which could activate caspase 3 (32 kDa) into a small fragment (17 kDa), which is the active form of caspase 3 and facilitates DNA fragmentation [37]. On cleavage of terminal caspases, such as caspase 3, cell death is generally thought to be inevitable. In our present study, levels of early mediators of apoptotic signalling proteins, such as Bcl-2 and Bax, showed significant differences in groups treated with NaHS and PAG. The downstream effectors like caspase 3 were significantly reduced in the NaHS-treated model group, and H_2S could also reduce mitochondria cytochrome *c* release.

However, it is important to note that those lines of evidence, such as the so-called apoptosis-related factors and TUNEL of DNA fragmentation for apoptosis in cardiomyocytes, are mostly indirect, and EM has been proposed to be the preferred direct technique. In sum, H_2S could inhibit apoptosis of cardiac myocytes through the mitochondrial pathway to improve the survival and ventricular dysfunction in the developing HF model. We propose that H_2S could be a valuable pharmacological target for HF therapy.

FUNDING

The present study was mainly supported by research grants from the Natural Science Foundation of China [grant numbers 30772565, 30888002]; and the National 973 Project [grant numbers 2007CB512006, 2010CB912600].

REFERENCES

1 Hunt, S. A., Baker, D. W., Chin, M. H., Cinquergrani, M. P., Feldman, A. M., Francis, G. S., Ganiats, T. G., Glodstein, S., Gregoratos, G., Jessup, M. L. et al. (2002) ACC/AHA guidelines for the evaluation and management of chronic heart failure in the adult. J. Heart Lung Transplant. 21, 189–203
2 Yan, A. T., Yan, A. R. and Liu, P. P. (2005) Pharmacotherapy for chronic heart failure: evidence from recent clinical trials. Ann. Intern. Med. 142, 132–145
3 Nian, M., Lee, P., Khaper, N. and Liu, P. (2004) Inflammatory cytokines and postmyocardial infarction remodeling. Circ. Res. 94, 1543–1553
4 Movassagh, M. and Foo, R. S. (2008) Simplified apoptotic cascades. Heart Fail. Rev. 13, 111–119
5 Wang, R. (2002) Two's company, three's a crowd: can H_2S be the third endogenous gaseous transmitter? FASEB J. 16, 1792–1798
6 Zhao, W., Ndisang, J. F. and Wang, R. (2003) Modulation of endogenous production of H_2S in rat tissues. Can. J. Physiol. Pharmacol. 81, 848–853
7 Kamoun, P. (2004) Endogenous production of hydrogen sulfide in mammals. Amino Acids 26, 243–254
8 Zhu, Y. Z., Wang, Z. J., Ho, P., Loke, Y. Y., Zhu, Y. C., Huang, S. H., Tan, C. S., Whiteman, M., Lu, J. and Moore, P. K. (2007) Hydrogen sulfide and its possible roles in myocardial ischemia in experimental rats. J. Appl. Physiol. 102, 261–268
9 Zhuo, Y., Chen, P. F., Zhang, A. Z., Zhong, H., Cheng, C. Q. and Zhu, Y. Z.(2009) Cardioprotective effect of hydrogen sulfide in ischemic reperfusion experimental rats and its influence on expression of survivin gene. Biol. Pharm. Bull. 32, 1406–1410
10 Chen, C. Q., Xin, H. and Zhu, Y. Z. (2007) Hydrogen sulfide: third gaseous transmitter, but with great pharmacological potential. Acta Pharmacol. Sin. 28, 1709–1716
11 Zhu, Y. Z., Zhu, Y. C., Li, J., Schafer, H., Schmidt, W., Yao, T. and Unger, T. (2000) Effects of losartan on haemodynamic parameters and angiotensin receptor mRNA levels in rat heart after myocardial infarction. J. Renin Angiotensin Aldosterone Syst. 1, 257–262
12 Ji, X. Y., Tan, B. K. H., Zhu, Y. C., Linz, W. and Zhu, Y. Z. (2003) Comparisons of cardioprotective effects using ramipril and Dansen for the treatment of acute myocardial infarction in rats. Life Sci. 73, 1413–1426
13 Mok, Y. Y., Atan, M. S., Yoke, P. C., Zhong, J. W., Bhatia, M., Moochhala, S. and Moore, P. K. (2004) Role of hydrogen sulphide in haemorrhagic shock in the rat: protective effect of inhibitors of hydrogen sulphide biosynthesis. Br. J. Pharmacol. 143, 881–889
14 Li, L., Bhatia, M., Zhu, Y. Z., Zhu, Y. C., Ramnath, R. D., Wang, Z. J., Binte Mohammed Anuar, F., Whiteman, M., Salto Tellez, M. and Moore, P. K. (2005) Hydrogen sulfide is a novel mediator of lipopolysaccharide-induced inflammation in the mouse. FASEB J. 19, 1196–1198
15 Geng, B., Chang, L., Pan, C., Qi, Y., Zhao, J., Pang, Y., Du, J. and Tang, C. (2004) Endogenous hydrogen sulfide regulation of myocardial injury induced by isoproterenol. Biochem. Biophys. Res. Commun. 318, 756–763
16 Du, J., Yan, H. and Tang, C. (2003) Endogenous H_2S is involved in the development of spontaneous hypertension. Beijing Da Xue Xue Bao 35, 102
17 Kimura, H. (2002) Hydrogen sulfide as a neuromodulator. Mol. Neurobiol. 26, 13–19
18 Whiteman, M., Armstrong, J. S., Chu, S. H., Jia, L. S., Wong, B. S., Cheung, N. S., Halliwell, B. and Moore, P. K. (2004) The novel neuromodulator hydrogen sulfide: an endogenous peroxynitrite 'scavenger'? J. Neurochem. 90, 765–768
19 Hosoki, R., Matsuki, N. and Kimura, H. (1997) The possible role of hydrogen sulfide as an endogenous smooth muscle relaxant in synergy with nitric oxide. Biochem. Biophys. Res. Commun. 237, 527–531
20 Zanardo, R. C., Brancaleone, V., Distrutti, E., Fiorucci, S., Cirino, G. and Wallace, J. L. (2006) Hydrogen sulfide is an endogenous modulator of leukocyte-mediated inflammation. FASEB J. 20, 2118–2120
21 Geng, B., Yang, J., Qi, Y., Zhao, J., Pang, Y., Du, J. and Tang, C. (2004) H_2S generated by heart in rat and its effects on cardiac function. Biochem. Biophys. Res. Commun. 313, 362–368
22 Reiffenstein, R. J., Hulbert, W. C. and Roth, S. H. (1992) Toxicology of hydrogen sulfide. Annu. Rev. Pharmacol. Toxicol. 32, 109–134
23 Mulder, P., Devaux, B., Richard, V., Henry, J. P., Wimart, M. C., Thibout, E., Mace, B. and Thuillez, C. (1997) Early versus delayed angiotensin converting enzyme inhibition in experimental chronic heart failure. Circulation 95, 1314–1319
24 Wang, X., Bing, R., Liu, S. Y., Sentex, E. and Tappia, P. S. (2003) Characterization of cardiac hypertrophy and heart failure due to volume overload in the rat. J. Appl. Physiol. 94, 752–763
25 Breckenridge, R. (2010) Heart failure and mouse model. Dis. Model Mech. 3, 138–143
26 Fliss, H. and Gattinger, D. (1996) Apoptosis in ischemic and reperfused rat myocardium. Circ. Res. 79, 949–956
27 Jeremias, I., Kupatt, C., Martin Villalba, A., Habazettl, H., Schenkel, J., Boekstegers, P. and Debatin, K. M. (2000) Involvement of CD95/Apo1/Fas in cell death after myocardial ischemia. Circulation 102, 915–920
28 Lee, P., Sata, M., Lefer, D. J., Factor, S. M., Walsh, K. and Kitsis, R. N. (2003) Fas pathway is a critical mediator of cardiac myocyte death and MI during ischemia-reperfusion *in vivo*. Am. J. Physiol. Heart Circ. Physiol. 284, H456–H463
29 Foo, R. S., Mani, K. and Kitsis, R. N. (2005) Death begets failure in the heart. J. Clin. Invest. 115, 565–571
30 Chatterjee, S., Stewart, A. S., Bish, L. T., Jayasankar, V., Kim, E. M., Pirolli, T., Burdick, J., Woo, Y. J., Gardner, T. J. and Sweeney, H. L. (2002) Viral gene transfer of the antiapoptotic factor Bcl-2 protects against chronic postischemic heart failure. Circulation 106, I212–I217
31 Chatterjee, S., Bish, L. T., Jayasankar, V., Stewart, A. S., Woo, Y. J., Crow, M. T., Gardner, T. J. and Sweeney, H. L. (2003) Blocking the development of postischemic cardiomyopathy with viral gene transfer of the apoptosis repressor with caspase recruitment domain. J. Thorac. Cardiovasc. Surg. 125, 1461–1469

32 Wencker, D., Chandra, M., Nguyen, K., Miao, W., Garantziotis, S., Factor, S. M., Shirani, J., Armstrong, R. C. and Kitsis, R. N. (2003) A mechanistic role for cardiac myocyte apoptosis in heart failure. J. Clin. Invest. 111, 1497–1504
33 Crow, M. T., Mani, K., Nam, Y. J. and Kitsis, R. N. (2004) The mitochondrial death pathway and cardiac myocytes apoptosis. Circ. Res. 95, 957–970
34 Narula, J., Pandey, P., Arbustini, E., Haider, N., Narula, N., Kolodgie, F. D., Dal Bello, B., Semigran, M. J., Bielsa Masdeu, A., Dec, G. W. et al. (1999) Apoptosis in heart failure: release of cytochrome *c* from mitochondria and activation of caspase-3 in human cardiomyopathy. Proc. Natl. Acad. Sci. U.S.A. 96, 8144–8149
35 Elrod, J. W., Calvert, J. W., Morrison, J., Doeller, J. E., Kraus, D. W., Tao, L., Jiao, X., Scalia, R., Kiss, L., Szabo, C. et al. (2007) Hydrogen sulfide attenuates myocardial ischemia-reperfusion injury by preservation of mitochondrial function. Proc. Natl. Acad. Sci. U.S.A. 104, 15560–15565
36 Communal, C., Sumandea, M., de Tombe, P., Narula, J., Solaro, R. J. and Hajjar, R. J. (2002) Functional consequences of caspase activation in cardiac myocytes. Proc. Natl. Acad. Sci. U.S.A. 99, 6252–6256
37 Baines, C. P. and Molkentin, J. D. (2005) Stress signaling pathways that modulate cardiac myocyte apoptosis. J. Mol. Cell. Cardiol. 38, 47–62

Received 7 January 2010/6 April 2010; accepted 7 May 2010
Published as Immediate Publication 7 May 2010, doi 10.1042/BSR20100003

